Design of All-Speed-Range Electronic Differential System for Front-Wheel-Independent-Drive Electric Vehicles

Bo-Chiuan Chen, Yen-Ju Huang, Shih-Hao Chen

National Taipei University of Technology, Taipei, Taiwan

E-mail: bochen@ntut.edu.tw

ABSTRACT: An all-speed-range electronic differential system (EDS) based on steering geometry during yaw motion is proposed for electric vehicles with front-wheel-independent-drive architecture and no mechanical differential. The EDS primarily calculates the reference wheel speeds for each driving wheel based on the desired vehicle speed and the steering angle, and subsequently generates the required motor drive torques through a wheel speed controller. To maintain the same steering feel, a feedforward compensation control is designed and integrated into the electric power steering system to adjust the assisting torque. Simulation results show that the proposed EDS can enhance vehicle handling and driving stability in various test scenarios and vehicle speeds.

KEY WORDS: all-speed-range, electronic differential, electric vehicles, front-wheel-independent-drive

1. INTRODUCTION

Electric vehicle drivetrains can be classified into centralized motor drive and independent wheel motor drive. During cornering, each wheel requires different torque and speeds. Centralized motor drive needs a mechanical differential to distribute torque, leading to efficiency losses due to multiple power transmissions. In contrast, independent wheel motor drive directly reduces transmission losses and allows more flexible control strategies. During cornering, motor torques can be allocated to each wheel to achieve the function of an electric differential system (EDS).

The Ackermann geometry can be used to calculate the reference wheel speeds for the inner and outer drive wheels [1, 2] to achieve the EDS function. This kind of approach does not use a yaw rate sensor. Thus, it cannot ensure yaw rate tracking performance when subjected to disturbances. In addition, the Ackerman geometry is only valid at low vehicle speeds. The turning center actually moves forward for medium and high vehicle speeds.

Direct yaw moment control (DYC) can be used to generate the virtual yaw moment control command for the yaw rate following [3, 4] to achieve the EDS function. However, control allocation is required to generate motor torque commands for each wheel [5-9]. Additionally, DYC is often designed based on a bicycle model, which is valid at medium and high vehicle speeds due to the characteristics of the lateral tire forces.

The above approaches do not consider steering torque variations caused by EDS or DYC. Asperti et al. [10] noted that the distribution of motor torques on the front wheels causes an unbalanced longitudinal force on the front wheels, resulting in an interference torque on the steering wheel, which affects driving feel and increases handling difficulty.

In this paper, a full-speed-range EDS based on a kinematics model is proposed with the consideration of steering geometry during yaw motion. A feedforward compensation control is also designed and integrated into the electric power steering (EPS) system to adjust the assisting torque to maintain the driver's steering feel similar to that of a rear-wheel drive electric vehicle.

2. CONTROLLER DESIGN

The control architecture proposed in this paper, as shown in Fig. 1, mainly consists of a reference generator and a wheel speed controller. The reference generator is responsible for calculating the reference wheel speed commands for the front drive wheels, while the wheel speed controller generates the corresponding drive torque to provide propulsion for the vehicle.

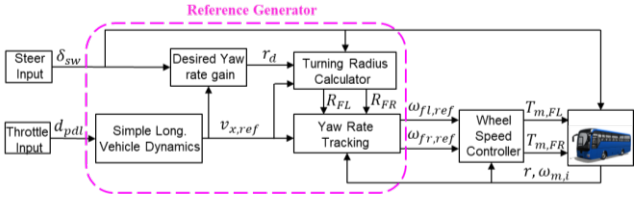

Fig. 1 Proposed control structure.

Similar to the EDS in [1], simple longitudinal vehicle dynamics is used to generate the desired vehicle speed $v_{x,ref}$ with the driver's throttle input d_{pdl}. The desired yaw rate r_d can then be

obtained by multiplying the steering input δ_f and the desired yaw rate gain which is designed as a function of $v_{x,ref}$. However, instead of using the Ackerman geometry with the point O as the turning center at low vehicle speeds as shown in Fig. 2, the steering geometry during yaw motion is used to derive the turning radiuses of the front wheels. As the vehicle speed increases, the front and rear wheels begin to experience lateral tire slip due to the influence of centrifugal force, causing the turning center to move from the point O to the point O'. The turning radiuses of the front left and front right wheels, i.e. R_{FL} and R_{FR}, can be obtained as follows.

$$R_{FL} \cong \sqrt{\left(R' - sign(\delta_f)\frac{d}{2}\right)^2 + {l_x}^2} \quad (1)$$

$$R_{FR} \cong \sqrt{\left(R' + sign(\delta_f)\frac{d}{2}\right)^2 + {l_x}^2} \quad (2)$$

where δ_f is the front wheel steering angle; d is the track width; R' and l_x are expressed as follows.

$$R' = \frac{L}{tan(\delta_f - \alpha_f) + tan(\alpha_r)} \quad (3)$$

$$l_x = \frac{L\,tan(\delta_f - \alpha_f)}{tan(\delta_f - \alpha_f) + tan(\alpha_r)} \quad (4)$$

where L is the wheelbase; α_f and α_r are the tire slip angles of the front and rear wheels, respectively.

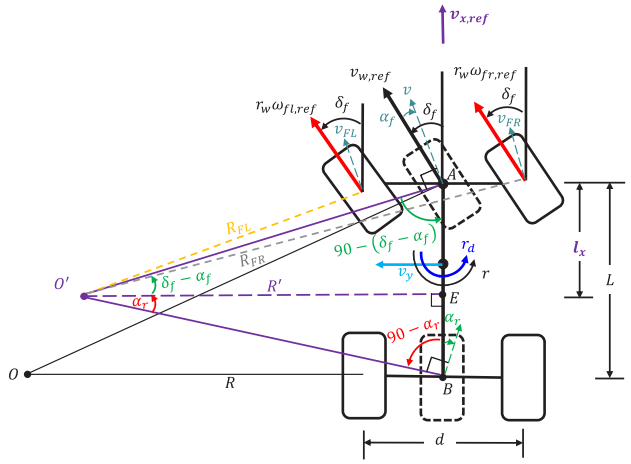

Fig. 2 Steering geometry during yaw motion.

After obtaining the turning radiuses of the front wheels, i.e. R_{FL} and R_{FR}, we can calculate the corresponding feed-forward wheel speed commands $\omega_{fl,FF}$ and $\omega_{fr,FF}$. To achieve yaw rate tracking, a closed-loop feedback control is designed to obtain the reference wheel speed commands $\omega_{fl,ref}$ and $\omega_{fr,ref}$. The overall architecture of yaw rate tracking control is illustrated in Fig. 3.

Adaptive RST control is employed to design the wheel speed controller as shown in Fig. 4. The subscript i denotes the front left or right wheel. During the control process, the lumped system

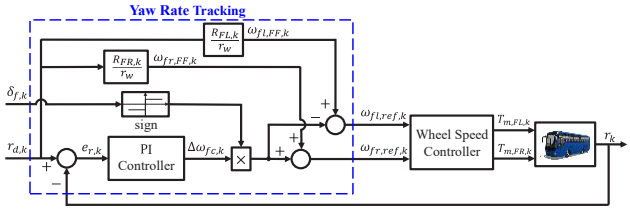

Fig. 3 Yaw rate tracking control.

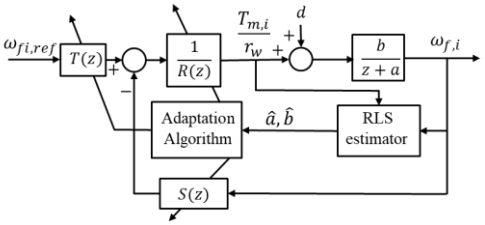

Fig. 4 Adaptive RST control.

parameters a and b are updated via the recursive least square method, and the coefficients of $R(z)$, $S(z)$, and $T(z)$ are adaptively adjusted according to time-varying system parameters.

3. STEERING FEEL COMPENSATION

When unequal driving forces act on the left and right front wheels, they create a steering torque on the steering column in addition to the EPS assist torque. The driver's steering feel is affected as shown in Fig. 5. Baseline denotes the steering feel of the rear-wheel-drive vehicle with a centralized traction motor and a mechanical differential. With the additional steering torque caused by the EDS, the increase in the steering angle does not correspond to a linear increase in the driver's steering torque SWT when the steering wheel angle SWA is between 30° and 50°.

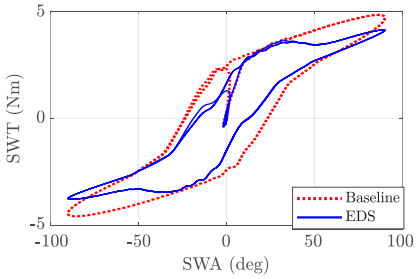

Fig. 5 Steering feel responses without compensation.

A feedforward compensation is proposed to restore the driver's steering feel as shown in Fig. 6. When the driver turns the steering wheel, the EPS generates a corresponding steering assist control command based on the required torque and the vehicle speed, using a two-dimensional lookup table. This command T_{EPS} first deducts the steering torque T_{EDS} generated by the EDS as shown below. The remaining part is provided by the EPS motor to assist the driver in cornering.

$$T_{EDS} = T_{EDS,R} - T_{EDS,L} \quad (5)$$

where $T_{EDS,R}$ and $T_{EDS,L}$ are the steering torques generated by the longitudinal tire forces of the front right and left wheels, i.e. $F_{x,FR}$ and $F_{x,FL}$, on the kingpin [11] which includes the factors of caster angle, scrub radius, camber angle, and the gear ratio between the front wheels and the steering wheel.

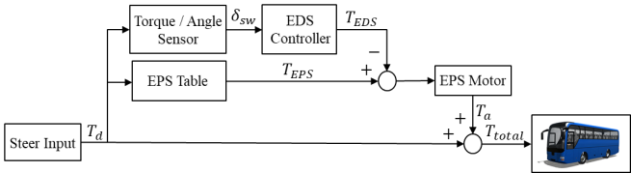

Fig. 6 Steering feel compensation.

After adding feedforward compensation, tests are conducted using the same scenario as shown in Fig. 7. The feedforward compensation significantly improves the driver's steering feel by reducing the EPS assist torque since the EDS itself also provides steering assist. This results in a more linear relationship between steering wheel angle and torque similar to that of Baseline.

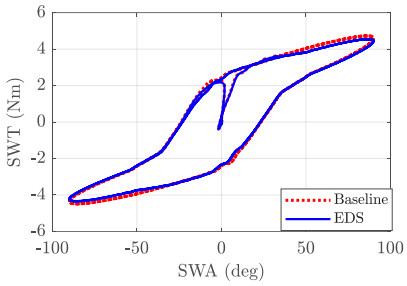

Fig. 7 Steering feel responses with compensation.

4. SIMULATION RESULTS

MATLAB/Simulink and TruckSim are utilized to construct the control architecture and simulate vehicle dynamics, respectively. Three strategies of Proposed, Even Dist., and Ackermann are evaluated using constant-radius circular and double lane-change tests. Even Dist. denotes evenly distributed front-wheel torques. Ackermann denotes the EDS based on the Ackermann geometry to distribute front-wheel drive torques.

4.1. Constant-radius Circular Test

Constant-radius (CR) circular tests using left turns are primarily conducted at speeds of 20 km/h, 40 km/h, 60 km/h, 80 km/h, and 100 km/h, with different turning radiuses used at each speed.

The vehicle dynamic responses at 40 km/h are shown in Fig. 8. Responses at other speeds are similar to those at 40 km/h. It can be seen that the proposed controller shows the smallest body slip angle β, steering wheel angle δ_{sw}, and yaw rate tracking error, indicating that the proposed EDS can achieve better yaw tracking performance and lateral stability.

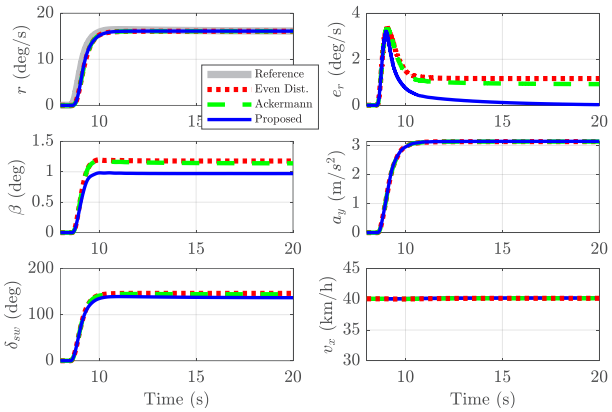

Fig. 8 CR responses of vehicle dynamics at 40 km/h.

The responses of wheel speeds and torque distributions are shown in Fig. 9. The proposed EDS increases the speed of the outer wheel and decreases the speed of the inner wheel to follow the desired yaw rate command. Ackermann also shows similar speed responses to assist cornering. However, a steady-state error remains due to the lack of yaw rate tracking. The proposed EDS, through yaw rate tracking control, adjusts the reference wheel speed, reducing the tracking error and improving lateral stability.

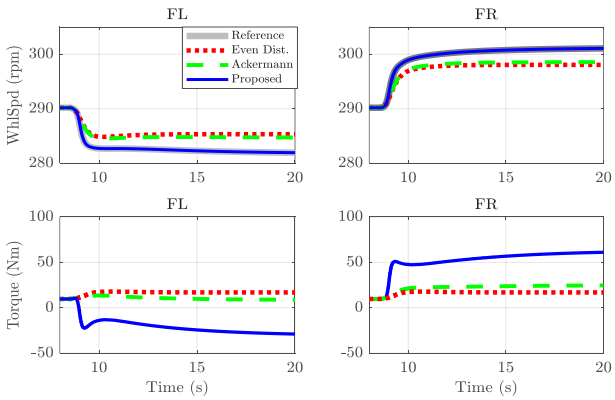

Fig. 9 CR responses of wheel speeds and torques at 40 km/h.

4.2. Double Lane-change Test

The vehicle cruises at a speed of 75 km/h on a high-friction road surface for the double lane-change (DLC) test. The trajectory responses are shown in Fig. 10. Since there is no longitudinal input from the driver, Even Dist. does not perform torque control. The proposed strategy can correct trajectory errors more quickly and achieve better path-following performance.

Responses of vehicle dynamics are shown in Fig. 11. The proposed EDS shows the smallest yaw rate tracking error e_r, body slip angle β, and steering wheel angle δ_{sw}. It significantly improves vehicle handling and stability, and allows the vehicle to maintain a straight-line driving quickly after completing the DLC.

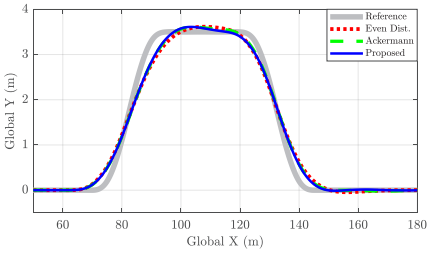

Fig. 10 Trajectory responses of DLC test.

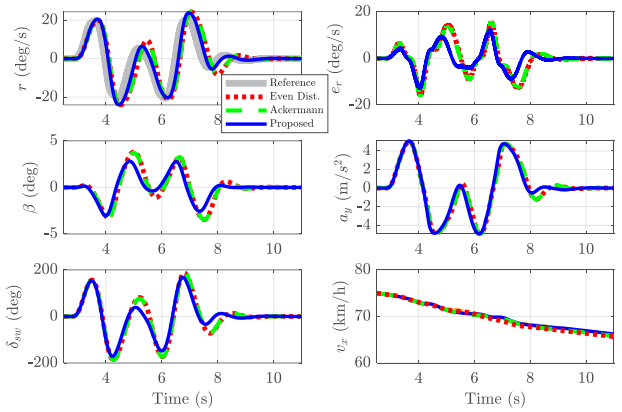

Fig. 11 DLC responses of vehicle dynamics at 75 km/h.

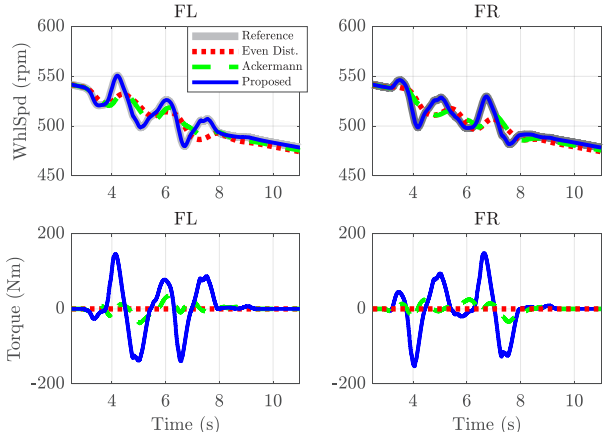

Fig. 12 DLC responses of wheel speeds and torques.

The response of wheel speeds and torque distributions are shown in Fig. 12. The proposed EDS can generate corresponding driving forces by following the reference wheel speed commands, ensuring good vehicle handling performance and stability. Although Ackermann is also effective at high speeds, it lacks yaw rate tracking control, resulting in worse dynamic responses similar to those of Even Dist.

5. CONCLUSIONS

An all-speed-range EDS is proposed for front-wheel-independent-drive electric vehicles. The reference command generator is designed based on the steering geometry during yaw motion to generate the required wheel speed commands for the front-drive wheels. The wheel speed controller based on adaptive RST control follows these commands to provide the necessary driving torques to the inner and outer wheels for cornering. Meanwhile, the feedforward compensation can restore the driver's steering feel. Simulation results show that the proposed EDS effectively solves steering feel issues and improves handling and lateral stability in both CR circular and DLC tests.

ACKNOWLEDGMENT

This research is sponsored by Cheng Yun Automobile Manufacturing Co., Ltd. We are deeply grateful for their financial support that made this study possible.

REFERENCES

(1) B.-C. Chen, C.-C. Yu, W.-S. Lee, and W.-F. Hsu, "Design of an Electric Differential System for Three-Wheeled Electric Welfare Vehicles With Driver-in-the-Loop Verification," *IEEE Transactions on Vehicular Technology*, vol. 56, no. 4, pp. 1498-1505, 2007.

(2) K. Hartani, M. Bourahla, Y. Miloud, and M. Sekour, "Electronic differential with direct torque fuzzy control for vehicle propulsion system," *Turkish Journal of Electrical Engineering and Computer Sciences*, vol. 17, no. 1, pp. 21-38, 2009.

(3) M. Nagai, Y. Hirano, and S. Yamanaka, "Integrated control of active rear wheel steering and direct yaw moment control," *Vehicle System Dynamics*, vol. 27, no. 5-6, pp. 357-370, 1997.

(4) S. Sakai and Y. Hori, "Robustified model matching control for motion control of electric vehicle," *in International Workshop on Advanced Motion Control*, pp. 574-579, 1998.

(5) H. Wei, Q. Ai, W. Zhao, and Y. Zhang, "Modelling and experimental validation of an EV torque distribution strategy towards active safety and energy efficiency," *Energy*, vol. 239, pp. 1-20, 2022.

(6) Z. Shuai, H. Zhang, J. Wang, J. Li, and M. Ouyang, "Lateral motion control for four-wheel-independent-drive electric vehicles using optimal torque allocation and dynamic message priority scheduling," *Control Engineering Practice*, vol. 24, no. 1, pp. 55-66, 2014.

(7) O. Mokhiamar and M. Abe, "Simultaneous optimal distribution of lateral and longitudinal tire forces for the

model following control," *Journal of Dynamic Systems, Measurement and Control*, vol. 126, no. 4, pp. 753-763, 2004.

(8) S. Xu, L. Wei, X. Zhang, Z. Bai, and Y. Jiao, “Research on Multi-Mode Drive Optimization Control Strategy of Four-Wheel-Drive Electric Vehicles with Multiple Motors,” *Sustainability*, vol. 14, no. 12, Art. no. 12, Jan. 2022.

(9) M. Kissai, B. Monsuez, X. Mouton, D. Martinez, and A. Tapus, "Model Predictive Control Allocation of Systems with Different Dynamics," *in 2019 IEEE Intelligent Transportation Systems Conference*, pp. 4710-4177, 2019.

(10) M. Asperti, M. Vignati, and E. Sabbioni, "Driver-in-the-Loop Simulation to Assess Steering Torque Feeling due to Torque Vectoring Control," *in 2022 IEEE Vehicle Power and Propulsion Conference*, 1-4 Nov. 2022, pp. 1-6, 2022.

(11) L. Filipozzi, E. Velenis, and F. Assadian, "Minimization of steering corruption during front axle torque vectoring," *in 2018 European Control Conference*, 12-15 Jun. 2018, pp. 673-678, 2018.